

Diffusive Shock Acceleration of High Energy Cosmic Rays

Matthew G. Baring^{a*}

^aDepartment of Physics and Astronomy, MS-108
Rice University, P. O. Box 1892,
Houston, TX 77251-1892, USA

The process of diffusive acceleration of charged particles in shocked plasmas is widely invoked in astrophysics to account for the ubiquitous presence of signatures of non-thermal relativistic electrons and ions in the universe. A key characteristic of this statistical energization mechanism is the absence of a momentum scale; astrophysical systems generally only impose scales at the injection (low energy) and loss (high energy) ends of the particle spectrum. The existence of structure in the cosmic ray spectrum (the "knee") at around 3000 TeV has promoted contentions that there are at least two origins for cosmic rays, a galactic one supplying those up to the knee, and even beyond, and perhaps an extragalactic one that can explain even the ultra-high energy cosmic rays (UHECRs) seen at 1-300 EeV. Accounting for the UHECRs with familiar astrophysical sites of acceleration has historically proven difficult due to the need to assume high magnetic fields in order to reduce the shortest diffusive acceleration timescale, the ion gyroperiod, to meaningful values. Yet active galaxies and gamma-ray bursts remain strong and interesting candidate sources for UHECRs, turning the theoretical focus to relativistic shocks. This review summarizes properties of diffusive shock acceleration that are salient to the issue of UHECR generation. These include spectral indices, acceleration efficiencies and timescales, as functions of the shock speed and mean field orientation, and also the nature of the field turbulence. The interpretation of these characteristics in the context of gamma-ray burst models for the production of UHECRs is also examined.

1. INTRODUCTION

The origin and nature of very high energy and ultra-high energy cosmic rays (UHECRs) continues to pique the interest of the physics and astrophysics communities. This topicality is driven by the lack of resolution of the apparent incompatibility of the data taken by the AGASA and Fly's Eye experiments at energies greater than around 6×10^{19} eV. Moreover, both these experiments and the Yakutsk initiative claim detections [37,16,55] of cosmic ray events above the so-called Greisen-Zatsepin-Kuzmin (GZK) cut-off, predicted by Greisen [36] and Zatsepin and Kuzmin [66]. This observational characteristic can place stringent constraints on both the seed for production of such energetic particles, and the sites in the Universe for their generation.

The UHECR paradigm is also underpinned by the existence of two competing scenarios for their creation: (i) the more conventional bottom-up

models, where the particles are accelerated from much lower energies up to the extreme values indicated by the air shower array data, and (ii) the generally newer and more exotic "top-down" possibilities that invoke creation and decay of various entities in particle physics that cascade down in energy to the GZK domain. Top-down scenarios have emerged as competitors to the more traditional bottom-up concepts since the latter have difficulty achieving energies in the 10^{20} eV range in most known astrophysical objects.

This review focuses on the properties of diffusive acceleration at relativistic shocks that are relevant to the production of UHECRs in astrophysical settings. These characteristics are not widely known outside the cosmic ray acceleration field. The viability of any putative source of UHECRs is contingent on its ability to generate particles of requisite energies in the available time, and with sufficient abundances and appropriate metallicity. Such quantities are sensitive to assumed parameters of shocks, such as field obliqu-

*Email: baring@rice.edu

uity, level of turbulence, the nature of scattering, and the role of accelerated particles in shaping the shock hydrodynamics. Subtle (and even not so obscure) implications of acceleration properties are often not addressed in bottom-up models for UHECRs that are offered for peer scrutiny, being left to specialist discussions within the acceleration community.

Here, the goal is to highlight some key properties of relativistic shock acceleration that are pertinent to various UHECR scenarios. To prepare the way, a few standard results from acceleration theory at non-relativistic shocks are briefly reviewed in Section 2, to facilitate comparison with the relativistic domain. This is the most-studied aspect of shock acceleration theory, with a number of very instructive reviews [23,17,41,50] in the literature. Moreover, it is the eminently testable domain, affording observational diagnostics via *in situ* spacecraft measurements [33,10] of accelerated populations at shocks in the heliosphere, and also numerous particle production and radiation models of supernova remnants (see [5] for a review), the principal contender for the sources of galactic cosmic rays. Section 3 then turns to the intricacies of relativistic shocks, focusing on several characteristics that distinguish them from their non-relativistic counterparts. A discussion of the impact of these properties on the gamma-ray burst (GRB) paradigm for UHECR production is offered in Section 4.

2. NON-RELATIVISTIC SHOCK ACCELERATION THEORY

The theory of diffusive acceleration of particles at non-relativistic shocks (those with upstream fluid speeds $u_1 \ll c$ in the shock rest frame) has been thoroughly investigated by both analytic and simulation techniques. The process, also known as Fermi acceleration, proceeds by particles being transported back and forth across a shock between colliding fluid flows. The kinematics of momentum deflections then yields a net energy gain, and the process can continue for a large number of shock crossings to generate high energy cosmic rays before they are lost due to convection, upstream escape, or even cooling. Much

is understood about this process, though the key outstanding issue is how electrons and ions are heated in the shock layer, and subsequently injected into the diffusive acceleration process. It is instructive to review three basic characteristics of $u_1 \ll c$ shocks to set the scene for the relativistic considerations of Section 3.

2.1. Canonical Index

Non-relativistic shocks generate particles with a power-law distribution in momentum. This is a consequence of high energy particles (those with speeds $v \gg u_1$) attaining isotropy in all pertinent reference frames, so that the so-called *diffusion approximation* can be applied. At such energies, the principal transport equation describing the acceleration process, the diffusion-convection equation, can be solved analytically for plane shocks [19,41], yielding the well-known result for the momentum distribution

$$\frac{dn}{dp} \propto p^{-\sigma} \quad \text{with} \quad \sigma = \frac{r+2}{r-1}, \quad (1)$$

where $r = u_1/u_2$ is the shock (velocity) compression ratio, p is the momentum. Eq. (1) is a steady-state, test-particle result. In this limit, the spectral index, σ , is independent of the shock speed, u_1 , the field obliquity, and any details of the scattering process as long as isotropy of highly super-thermal particles is maintained. The canonical nature of this result is a driving force behind invocations of acceleration in astrophysics. Note that a high Mach number, non-relativistic shock has $r \approx 4$ and $dn/dp \propto p^{-2}$.

2.2. The Character of Oblique Shocks

The result in Eq. (1) exhibits no information concerning the normalization of the power-law. Such a property is controlled by the rate at which particles are injected from thermal energies. This injection rate is sensitive to the angle Θ_{Bn1} the mean upstream magnetic field makes to the shock normal. In the downstream region, particles are swept away more efficiently from the shock by the convective force of the flow when the obliquity angle Θ_{Bn1} is higher. For non-relativistic shocks of high Mach number, when $\Theta_{\text{Bn1}} \gtrsim 30^\circ$, the convection is so effective that injection of thermal particles into the acceleration process is entirely

suppressed [8]. The critical angle at which acceleration ceases increases to around $\Theta_{\text{Bn1}} \sim 55^\circ$ for hotter, low Mach number shocks. These results apply if the diffusion is dominant along the magnetic field, i.e. the ratio $\kappa_{\perp}/\kappa_{\parallel}$ of spatial diffusion coefficients κ_{\parallel} along the field and κ_{\perp} orthogonal to \mathbf{B} is much less than unity. Here $\kappa_{\parallel,\perp} = \lambda_{\parallel,\perp}v/3$ for scattering mean free paths $\lambda_{\parallel,\perp}(v)$, for particle speeds v . A concomitant effect of obliquity is the dramatic increase in the acceleration rate [39,57] in highly oblique shocks, above the $\Theta_{\text{Bn1}} = 0^\circ$ values [34] that can be inferred from Eq. (2) below. This increase can be ascribed to the presence of electric fields in the shock layer that seed shock-drift acceleration.

While the rapid reduction of the acceleration time in oblique and quasi-perpendicular shocks is enticing, the inefficient acceleration is unattractive to cosmic ray production models. This trade-off is an unavoidable property of oblique shocks [26]. Restricting to $\kappa_{\perp} \ll \kappa_{\parallel}$ cases is not always appropriate. Increasing κ_{\perp} , physically corresponding to stronger field turbulence, tends to eliminate laminarity information in the field and accordingly renders the shock more like a parallel, $\Theta_{\text{Bn1}} \sim 0^\circ$ one. Consequently, increasing κ_{\perp} towards the Bohm limit of $\kappa_{\perp} \sim \kappa_{\parallel}$ mutes the increases in acceleration rates, and returns injection efficiencies to levels commensurate with plane-parallel shocks [26]. Modelers therefore must compromise: either opt for quasi-laminar oblique shocks that are faster but less efficient accelerators, or extremely turbulent shocks of arbitrary obliquity that generate cosmic rays efficiently but at standard rates, i.e. the inverse gyrofrequency corresponding to a specific particle energy.

2.3. Nonlinear Modifications

The aforementioned features apply to circumstances where the accelerated particles do not modify the shock hydrodynamics, i.e. are dynamically unimportant and act as test particles. Yet, when acceleration is extremely efficient, a sizable fraction of the total energy budget emerges as high energy cosmic rays, an inevitable occurrence in an $r \approx 4$ shock if the power-law in Eq. (1) extends to high enough energies. The pressure of these particles decelerates the upstream flow,

which in turn provides feedback to the distribution of accelerated ions and electrons, and therefore the fraction of energy going into these particles. This nonlinearity has been thoroughly explored in the literature [24,23,25,31,27,15,49,20] and is a critical characteristic of efficient shocks. The quintessential example is the Earth's bow shock immersed in the solar wind; it affords a nice data comparison between experiment and acceleration theory [33].

As a result of the energy conservation that regulates the acceleration and the energy apportionment between thermal ions and high energy cosmic rays, there are two distinctive features of nonlinear, cosmic ray modified shocks: (i) a distribution that deviates from pure power-law nature, exhibiting a characteristic upward concavity due to higher energy particles sampling larger effective compression ratios, since their diffusive mean free paths are longer, and (ii) the thermal particles are somewhat cooler [14] than for test-particle shocks, since the subshock is weakened and energy removed from the thermal ions and electrons. These phenomena can be probed to a certain extent by examining isolated, radiating systems such as supernova remnants, and at present, there are at best modest indications to support these theoretical predictions.

3. DISTINGUISHING PROPERTIES OF RELATIVISTIC SHOCKS

Diffusive acceleration at relativistic shocks is far less studied than that for non-relativistic flows, yet it is a most applicable process for UHECR generation, and may occur in extreme objects such as pulsar winds, hot spots in radio galaxies, jets in active galactic nuclei and microquasars, and GRBs. Early work on relativistic shocks was mostly analytical in the test-particle approximation (e.g., [59,45,38,47]), although the analytical work of [60,9] explored nonlinear, cosmic ray modified shocks. Complementary Monte Carlo techniques have been employed for relativistic shocks by a number of authors, including test-particle analyses by [46,32] for parallel, steady-state shocks, and extensions to include oblique magnetic fields by [58,3,13].

A key characteristic that distinguishes relativistic shocks from their non-relativistic counterparts is their inherent anisotropy due to rapid convection of particles through and away downstream of the shock, since particle speeds v are never much greater than the downstream flow speed $u_2 \sim c/3$. Accordingly, the diffusion approximation, the starting point for virtually all analytic descriptions of shock acceleration when $u_1 \ll c$, cannot be invoked since it requires nearly isotropic distribution functions. Hence analytic approaches prove more difficult when $\gamma_1 \gg 1$, though advances in special cases such as the limit of extremely small angle scattering (*pitch angle diffusion*) are possible [45,44]. Let us explore some of the distinctive properties of particle acceleration at relativistic shocks.

3.1. Non-Universality of the Spectrum

The most attractive feature of non-relativistic shock acceleration theory is that the distribution of accelerated particles is scale-independent, i.e. a power-law, as in Eq. (1), with an index σ that depends only on the velocity compression ratio $r = u_1/u_2$, i.e. hydrodynamic quantities. This elegant result does not carry over to relativistic shocks because of their strong plasma anisotropy. As a consequence, while power-laws are indeed created, the index σ becomes a function of the flow speed, the field obliquity, and the nature of the scattering, all of which intimately control the degree of particle anisotropy.

In the specific case of parallel, ultrarelativistic shocks, the analytic work of Kirk et al. [44] demonstrated that as $\Gamma_1 \rightarrow \infty$, the spectral index σ asymptotically approached a constant, $\sigma \rightarrow 2.23$, a value realized once $\Gamma_1 \gtrsim 10$. This enticing result, which has been confirmed by Monte Carlo simulations [13,4,1,28], has been referred to sometimes as an indication of the universality of the index in relativistic shocks. In this subsection, it is illustrated that the asymptotic index of 2.23 is indeed not canonical, but rather a special case corresponding to compression ratios of $r = 3$ and the particular assumption of small scattering (pitch angle diffusion), specifically for incremental changes θ_{scatt} in a particle's momentum with angle $\theta_{\text{scatt}} \ll 1/\Gamma_1$.

First, the spectral index of the power-law distribution is a declining function of the Lorentz factor for a fixed compression ratio, a characteristic evident in [45,2,44] for the case of pitch angle scattering, and a property that extends to large angle scattering [32,4]. Faster shocks generate flatter distributions if r is held constant, a consequence of the increased kinematic energization occurring at relativistic shocks. Note that imposing a specific equation of state such as the Jüttner-Synge one renders r a function of Γ_1 so that this monotonicity property can disappear, as evinced in Fig. 2 of Kirk et al. [44]. Table 1 lists indices σ of the dn/dp distribution obtained from the Monte Carlo simulation technique of Ellison et al. [32]. These results, obtained specifically in the limit of pitch angle diffusion, illustrate the flattening as Γ_1 increases.

Table 1
Spectral Indices σ for Pitch Angle Diffusion at Relativistic, Plane-Parallel Shocks.

$\Gamma_1 \beta_1^a$	$r = 2$	$r = 2.5$	$r = 3$	$r = 3.5$	$r = 4$
30	3.24	2.57	2.23	1.99	1.86
10	3.28	2.59	2.23	2.00	1.87
3	3.33	2.64	2.26	2.02	1.86
2	3.38	2.67	2.28	2.03	1.88
1	3.48	2.72	2.31	2.05	1.89
0.3	3.90	2.95	2.42	2.15	1.96
0.1	3.96	2.98	2.46	2.17	1.98
0.03 ^b	3.98	2.99	2.49	2.19	1.99

The spectral indices are from the Monte Carlo simulation of [32], and the accuracy of their determination is typically of the order of ± 0.02 . Notes: (a) Here $\beta_1 = u_1/c$ and Γ_1 are the dimensionless velocity and Lorentz factor of the upstream flow in the shock rest frame, respectively. (b) This non-relativistic limit approximately reproduces the well-known $\sigma = (r + 2)/(r - 1)$ result in Eq. (1).

The choice of the canonical compression ratio $r = 3$ is a well-known result for a relativistic, purely hydrodynamic shock possessing an ultra-relativistic equation of state [18]. However, one

can envisage situations where the magnetic field becomes dynamically important. The classic example is the termination shock for the Crab pulsar wind, where Kennel & Coroniti [43] observed that strong fields can weaken magnetohydrodynamic shocks considerably. In an interesting generalization of this, Double et al. [22] recently determined deviations from $r = 3$ in ultrarelativistic shocks, in cases where pressure anisotropy is significant, a characteristic that is expected to be common in relativistic shocks. Such departures can either strengthen *or* weaken the shock depending on the nature of the pressure anisotropy, which must be a significant function of the shock obliquity, i.e., Θ_{Bn1} . Hence, we anticipate that σ will be a function Θ_{Bn1} , an issue visited again in this Section.

More novel is the fact that the slope of the non-thermal particle distribution depends on the nature of the scattering, a feature evident in the works of Refs. [32,13,4]. The asymptotic, ultrarelativistic index of 2.23 is realized only in the mathematical limit of pitch angle diffusion (PAD), where the particle momentum is stochastically deflected on arbitrarily small angular (and therefore temporal) scales. In practice, PAD results when the scattering angle θ_{scatt} is inferior to the Lorentz cone angle $1/\Gamma_1$ in the upstream region. In such cases, particles diffuse in the region upstream of the shock only until their angle to the shock normal exceeds around $1/\Gamma_1$. Then they are rapidly swept to the downstream side of the shock. The energy gain per shock crossing cycle is then of the order of a factor of two, simply derived from relativistic kinematics [35,4]. The spectrum, depicted in Fig. 1, is then slightly steeper than the p^{-2} result for a strong, non-relativistic shock, due to the balance between particle energization and loss by convection downstream.

The results in Fig. 1 are from the Monte Carlo simulation of acceleration at relativistic shocks developed by Ellison et al. [32], who demonstrated that for large angle scattering (LAS, with $\theta_{\text{scatt}} \sim \pi$) the spectrum is highly structured and much flatter than E^{-2} . Such a case is exhibited in the Figure. The structure is kinematic in origin, where large angle deflections lead to distribution of fractional energy gains between unity and

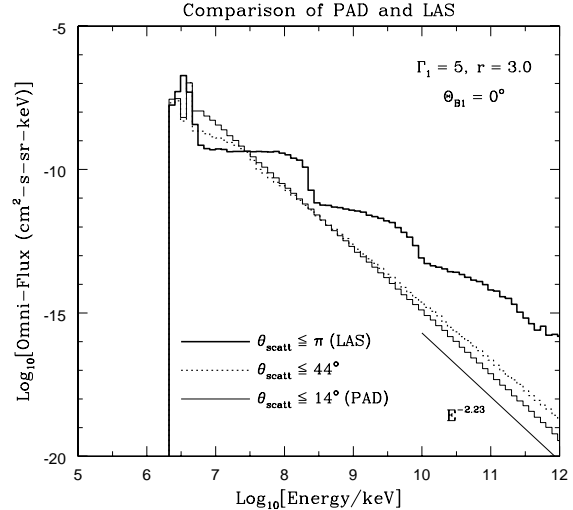


Figure 1. Particle distributions from a parallel ($\Theta_{\text{Bn1}} = 0$) relativistic shock of $r = 3$ and Lorentz factor $\Gamma_1 = 5$, obtained from a Monte Carlo simulation [32,4]. Scattering is modeled by randomly deflecting particle momenta by an angle θ_{scatt} within a cone whose axis coincides with the momentum prior to scattering. Distributions are depicted for three cases, $\theta_{\text{scatt}} \leq 14^\circ$, corresponding to pitch angle diffusion (PAD), large angle scattering (LAS: $\theta_{\text{scatt}} \leq \pi \gg 1/\Gamma_1$), and an intermediate case (dotted histogram).

Γ_1^2 . Gains like this are kinematically analogous to the energization of photons by relativistic electrons in inverse Compton scattering. Each structured bump or spectral segment in Fig. 1 corresponds to an increment in the number of shock crossings, successively from $1 \rightarrow 3 \rightarrow 5 \rightarrow 7$ etc., as illustrated by Baring [4], that eventually smooth out to asymptotically approach an index of $\sigma \sim 1.5$. Clearly, such highly-structured distributions have not been inferred from radiation emission in any astrophysical objects.

An intermediate case is also depicted in Fig. 1, with $\theta_{\text{scatt}} \sim 4/\Gamma_1$. The spectrum is smooth, like the PAD case, but the index is lower than 2.23. Astrophysically, there is no reason to exclude such cases. Moreover, from the plasma point of view, magnetic turbulence could easily be sufficient to effect scatterings on the order of these angles, a

contention that becomes even more salient for ultrarelativistic shocks with $\Gamma_1 \gg 10$. Note that the $\Gamma_1 = 5$ results depicted here are entirely representative of the nature of such ultrarelativistic cases. Clearly a range of indices can be supported when θ_{scatt} is chosen to be of the order of $1/\Gamma_1$, and the scattering corresponds to the transition between the PAD and LAS limits. It is anticipated that various astrophysical systems will encompass a range of scattering properties. Accordingly, the continuous and monotonically decreasing behavior of σ with θ_{scatt} , as indicated in the exposition of [29], highlights the non-universality of the distribution index in relativistic shocks.

Categorizing the scattering as either PAD or LAS is a useful division, but is not a complete description of diffusive transport in shocks. Another characteristic, the diffusion of particles across mean field lines, becomes a critical element in the discussion of oblique or perpendicular shocks. As mentioned above, when the upstream angle Θ_{Bn1} of the field to the shock normal is significant, diffusion of particles in the downstream region struggle to compete with convective losses, and transport back upstream of the shock layer becomes inefficient. In non-relativistic shocks, this effect was explored by Baring et al. [8], who observed that the losses controlled the injection efficiency of nonthermal particles, so that when $\Theta_{\text{Bn1}} \gtrsim 30^\circ$, thermal particles of speed $v \gtrsim u_1$ fail to return to the shock after one crossing to the downstream side and the Fermi acceleration process is quenched. Accordingly, for $\Theta_{\text{Bn1}} < 30^\circ$ in such regimes, while power-law superthermal distributions are exhibited, their normalization is a strongly declining function of Θ_{Bn1} when transport across field lines is suppressed.

This phenomenon is manifested in a somewhat different manner in relativistic shocks. When $u_1 \sim c$, the $v \gtrsim u_1$ criterion for dramatic, if not catastrophic, convective losses is satisfied for *all* particle speeds, not just slightly suprathermal ones. Hence such losses can be expected to be pervasive for all non-thermal energies. Increased losses must diminish the nonthermal population, and since the loss rate is purely a function of particle speed [59,41], which is effectively pinned at $v \approx c$, and u_2 , the net effect is to increase the

spectral index while retaining power-law character. This property is illustrated in Fig. 2, where the simulation output was acquired in the absence of cross field diffusion (i.e., $\kappa_\perp = 0$). Increasing Θ_{Bn1} results in a rapid rise in σ corresponding to a suppression of acceleration. Essentially, for $\Theta_{\text{Bn1}} \gtrsim 25^\circ$, acceleration is virtually non-existent for $\Gamma_1\beta_1 \gtrsim 1$.

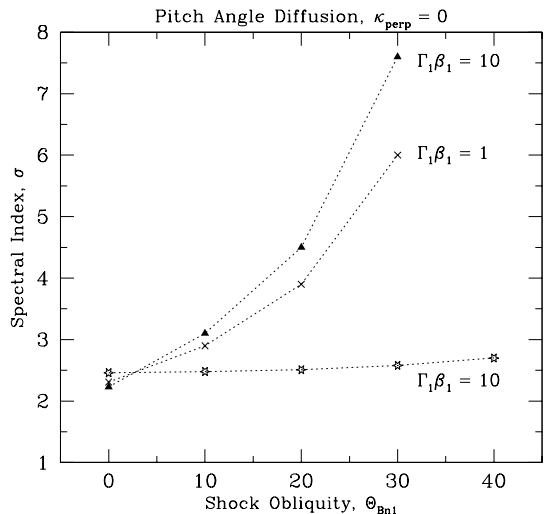


Figure 2. Particle distribution indices σ from oblique ($\Theta_{\text{Bn1}} > 0$) relativistic shocks of $r = 3$ and different Lorentz factors Γ_1 , obtained from a Monte Carlo simulation [32,4] in the limit of pitch angle diffusion. Results are depicted for the case of zero diffusive transport perpendicular to the mean field, i.e., $\kappa_\perp = 0$ for the perpendicular component of the spatial diffusion coefficient κ . The index is insensitive to Θ_{Bn1} for non-relativistic shocks, but rapidly increases with obliquity for relativistic ones, underlining their inherent inefficiency.

Turbulent plasmas in shock environs generally will not admit a $\kappa_\perp = 0$ assumption. Strong turbulence will drive the system towards the so-called *Bohm-diffusion* limit, where diffusion coefficients are similar parallel and perpendicular to the field, i.e. $\kappa_\perp \sim \kappa_\parallel$, and transport is effectively isotropic. Efficient transport across

field lines can to a significant extent circumvent convective losses, returning the particles to the shock from the downstream region, and accordingly flattening the power-law distribution. It is anticipated that transport near the Bohm limit would be essential to generate $\sigma \lesssim 3$, i.e. indices meaningful for UHECR acceleration paradigms. This is borne out in [13] and the recent work of Ellison & Double [29], who obtained $\sigma \approx 2.34$ for a $\Gamma_1 = 10$, $\Theta_{\text{Bn1}} = 60^\circ$ shock in the extreme case of the Bohm limit. The Monte Carlo simulation results of [13,29] also exhibited the expected monotonic decrease in σ with the increase in $\kappa_\perp/\kappa_\parallel$.

3.2. Acceleration Times

Having explored spectral issues germane to the UHECR problem, we now turn our attention to the maximum energy issue. This is essentially determined by the rate at which particles are accelerated, so diffusive acceleration times become the focal point. Various authors have researched this subject for relativistic shocks [32,12,11,1,6,52]. In particular, [32] found that for large angle scattering, the acceleration time for a $\Gamma_1 \lesssim 5$ shock was only marginally shorter than that expected from classical non-relativistic shock theory. The simulations of Bednarz & Ostrowski [12,11] revealed similar modest reductions for both LAS and PAD. Observe that in spite of substantial energy gains per shock crossing, typically on the order of Γ_1^2 , the particles then spend considerable time diffusing downstream, a time coupled to their inverse gyrofrequency.

Recently, Baring [6] computed acceleration times in the limit of pitch angle diffusion using the simulation of [32], specifically for application to jets in blazars. It was found that extrapolation of simulations into the relativistic regime revealed a hard lower bound on the total acceleration time τ_{acc} as measured in the shock rest frame. The time τ_{acc} monotonically decreases (for ultrarelativistic particles) to this limit as Γ_1 increases to infinity, yet proximity is achieved for $\Gamma_1 \gtrsim 10$. If ν_g represents the energy-dependent gyrofrequency of an ultrarelativistic electron or ion, then the velocity dependence of the acceleration times in plane-parallel shocks can be approximated (to

around 1–3% accuracy) by the empirical fit

$$\tau_{acc} \approx \left(\frac{1}{4} - \frac{0.18}{\Gamma_1 \beta_1} + \frac{1}{\Gamma_1^2 \beta_1^2} + \frac{0.22}{1 + \Gamma_1 \beta_1} \right) \tau_{\text{NR}} \quad (2)$$

$$\tau_{\text{NR}} \equiv \tau_{\text{NR}}(\beta_1 = 1) = \frac{f}{\nu_g} .$$

Here $\tau_{\text{NR}}(\beta_1 = 1)$ is the extrapolation of the well-known acceleration time formula [34,39] for non-relativistic, parallel shocks to flow speeds c . The times are for a velocity compression ratio of $u_1/u_2 = 3$, and the coefficient f describes details of the differences in diffusion between the upstream and downstream regions, and is of the order of unity and independent of Γ_1 . Note that when $\beta_1 \ll 1$, the familiar non-relativistic result emerges: $\tau_{acc} = \tau_{\text{NR}}/\beta_1^2$. Introducing shock obliquity can speed up the acceleration, as in non-relativistic cases, but at the price of dramatically steepening the distribution.

The bound arises due to the insensitivity of the downstream flow speed and diffusion in the downstream region to the upstream Γ_1 . Downstream diffusion yields the dominant contribution to τ_{acc} , with upstream particles requiring only small deflections (accomplished in short times: e.g., [11]) from the shock normal in order to return downstream. This automatically implies a hard lower bound to τ_{acc} as $\Gamma_1 \rightarrow \infty$, since the downstream speed saturates at $c/3$. Effectively, particles can never be accelerated at rates much faster than their gyrofrequency. The limit translates to a *comparable limit in the upstream fluid frame*, which is often the observer's reference perspective, for example the interstellar medium surrounding a jet. This property follows from the connection between Lorentz transformations of times and energies, with the proper time of the particle being a Lorentz invariant.

Hence, models of acceleration at relativistic shocks do not incur any increases to the energization rate other than the enhancement of the field by a single Lorentz boost. Maximum energies are then only explicitly weakly dependent on shock speeds. This implies that sites for cosmic ray acceleration generally must invoke higher environmental magnetic fields to effect higher maximum particle energies.

4. IMPACT ON UHECR PARADIGMS

As an illustrative and topical case, the focus here is on the scenario that gamma-ray bursts are sites for the generation of ultra-high energy cosmic rays. The discussion will emphasize acceleration issues, as opposed to source population considerations.

4.1. Gamma-Ray Burst Applications

The paradigm that gamma-ray bursts (GRBs) are responsible for UHECR production [54,65,63], has been quite topical over the last decade. Bursts are sufficiently energetic to amply satisfy cosmic ray energy budgets if their space density is not too sparse. Consequently the redshift distribution of GRBs, not well-known at present but soon to be refined by the SWIFT mission, is an important constraint [61] on the ability of bursts to serve as sites for UHECR generation. Given the level of community interest, it is salient to assess the aforementioned acceleration results in the context of gamma-ray bursts.

First, the discussions above indicate that the maximum energy of cosmic rays from bursts is not increased by subtle relativistic effects, and can be approximately estimated using standard non-relativistic shock theory with modification as per Eq. (2). It can be quickly deduced, by comparing the inverse gyrofrequency with subsecond burst variability timescales, that UHECRs can be generated in GRBs if the magnetic fields inside the burst are of the order of $B \sim 10^5 - 10^7$ G inside the emission region. This is not dissimilar from field estimates (e.g., [53,7]) obtained by synchrotron radiation modeling of their prompt gamma-ray emission in the MeV band, so approximate consistency is achieved. It is not yet understood how such large fields arise in GRB shocks, though ideas of field amplification at shocks [51,48] have recently become prominent.

The non-universality of the power-law index and its sensitivity to obliquity and the anisotropy of turbulent transport immediately indicate that GRB spectra should possess diverse indices. This should be manifested in the energy range above the 100 keV – 1 MeV peak of emission, and is in fact so in data taken from the EGRET experi-

ment on the Compton Gamma-Ray Observatory (CGRO), where the half dozen or so bursts seen at high energies have a broad range of spectral indices [21], namely $\alpha \sim 2 - 3.7$ for $dn/d\varepsilon_\gamma \propto \varepsilon_\gamma^{-\alpha}$. This result suffers from limited statistics due to (i) the nature of bursts, and (ii) to EGRET's field of view being more limited than that for BATSE, the principal GRB experiment on CGRO. The upcoming GLAST mission will provide a more refined determination of the distribution of burst indices above 30 MeV after its launch in 2007.

At the same time, in order to emit the radiation detected, GRBs must have underlying electron distributions that are relatively flat. By extension, since the electron and cosmic ray ion distributions trace each other in theories of shock acceleration where the diffusive mean free path is dependent only on rigidity, then the ion index must lie in the range $\sigma \sim 3 - 6$. This is a spectral constraint commensurate with that imposed by the observed E^{-3} UHECR distribution [64,55]. As the UHECR spectrum results from a convolution of a host of sources, modulo unknown propagation effects, one expects that the flatter distributions will dominate, so there is a satisfying consistency between UHECR ion and GRB photon spectra. Since GRB shocks are believed to be ultrarelativistic, the acceleration results discussed above (as exemplified in Fig. 2) indicate that strong cross field diffusion (i.e., $\kappa_\perp \sim \kappa_\parallel$) will be necessary in the majority of bursts, if their shocks are oblique, as is highly likely. This property is required to provide a cosmic ray distribution at least as flat as the observations, and indeed efficiently generate cosmic rays in sufficient numbers. Note that the same would apply to jets in active galaxies such as blazars, as an alternative source of UHECRs.

An acceleration issue not addressed above concerns the shape of the particle distributions at thermal and slightly suprathreshold energies. This is essentially an injection or dissipational heating issue that is readily probed for electrons by the spectrum of prompt GRB emission. Baring & Braby [7] pursued a program of spectral fitting of GRB emission using a linear combination of thermal and non-thermal electron populations. These fits demanded that the prepon-

derance of electrons that are responsible for the prompt emission reside in an intrinsically non-thermal population, strongly contrasting particle distributions obtained from acceleration simulations. This result implies a conflict for acceleration scenarios where the non-thermal electrons are drawn directly from a thermal gas (the virtually ubiquitous case), unless radiative efficiencies only become significant at highly superthermal energies. Another potential caveat is that strong radiative self-absorption could be acting, in which case the GRB spectral probe is not sampling the thermal electrons. Considerable work is needed to resolve this issue to ascertain whether an acceleration paradigm can be truly consistent with the GRB emission that is seen.

5. OUTLOOK

The UHECR field is clearly anticipating the next generation of observational data from the Auger experiment, just around the corner. In the meantime, theorists will continue to develop their models and hone their understanding. In terms of acceleration theory, at least two key developments can be expected in the coming years.

First, with the advent of rapidly increasing computational capability, reliance on analytic and Monte Carlo techniques is no longer essential, and these acceleration approaches will be supplanted in part by modeling by fully 3D plasma codes, namely particle-in-cell (PIC) simulations. Such simulations have generated interesting results in the last decade, but have been hampered [40,42] by restricted dimensionality imposed by CPU memory and speed limitations. In the last 2-3 years, results from 3D codes have achieved increasing visibility, particularly for modeling relativistic shocks [62,56]. Their key impediment is having to treat widely disparate inertial scales associated with the proton to electron mass ratio. Their virtue is the accurate modeling of particle heating, coherent acceleration effects and field amplification in the shock layer. One can expect many interesting developments and results from PIC codes in the coming decade.

Monte Carlo techniques will still continue to be powerful tools, due to their capability of handling

large dynamic ranges in spatial and momentum scales. Thus they are ideally suited to nonlinear acceleration scenarios, which can impact the interpretation of UHECR ion composition studies, since nonlinear non-relativistic systems are well-known to preferentially accelerate ions with higher mass to charge ratios [30]. The application of the Monte Carlo approach to nonlinear, relativistic shocks has so far been very limited [28], and this is territory ripe for investigation. It is anticipated that nonlinear effects will be more subtle for the $u_1 \sim c$ domain, since particle distributions are sensitive to the shock speed, obliquity and the type of scattering that operates. In addition, the shock hydrodynamics are dependent on the plasma anisotropy, and this is inextricably connected to u_1 , Θ_{Bn1} and θ_{scatt} also. Hence, research in the near future should focus on elucidating the interplay between these ingredients. Such simulations also need to explore ways to address injection and heating of thermal species in a more consistent manner, including the influence of electric potentials in the shock layer.

REFERENCES

1. Achterberg, A., et al. 2001, M.N.R.A.S. 328, 393.
2. Ballard, K. R. & Heavens, A. F. 1991, M.N.R.A.S. 251, 438.
3. Ballard, K. R. & Heavens, A. F. 1992, M.N.R.A.S. 259, 89.
4. Baring, M. G. 1999, in *Proc. of the 26th ICRC, Vol. IV*, p. 5, [astro-ph/9910128].
5. Baring, M. G. 2000, in *GeV-TeV Gamma-Ray Astrophysics Workshop*, eds. B. L. Dingus, et al. (AIP Conf. Proc. 515, New York), p. 173, [astro-ph/9911060]
6. Baring, M. G. 2002, Publ. Astron. Soc. Aust., 19, 60.
7. Baring, M. G. & Braby, M. L. 2004, ApJ in press (Sep. 20, 2004) [astro-ph/0406025]
8. Baring, M. G., Ellison, D. C. & Jones, F. C. 1994, ApJ Supp. 90, 547.
9. Baring, M. G. & Kirk, J. G. 1991, Astron. Astrophys. 241, 329.
10. Baring, M. G., Ogilvie, K. W., Ellison, D. C. & Forsyth, R. J. 1997, ApJ 476, 889.

11. Bednarz, J. 2000, M.N.R.A.S. 315, L37.
12. Bednarz, J. & Ostrowski, M. 1996, M.N.R.A.S. 283, 447.
13. Bednarz, J. & Ostrowski, M. 1998, Phys. Rev. Lett. 80, 3911.
14. Berezhko, E. G., & Ellison, D. C. 1999, ApJ 526, 385.
15. Berezhko, E. G., Yelshin, V. K. & Ksenofontov, L. T. 1996, JETP 82(1), 1.
16. Bird, D., et al. 1995, ApJ 441, L144.
17. Blandford, R. D. & Eichler, D. 1987, Phys. Rep. 154, 1.
18. Blandford, R. D. & McKee, C. F. 1976, Phys. Fluids 19 #8, 1130.
19. Blandford, R. D. & Ostriker, J. P. 1978, ApJ 221, L29.
20. Blasi, P. 2002, Astroparticle Phys. 16, 429.
21. Dingus, B. L. 1995, Astr. Space Sci. 231, 187.
22. Double, G. P., Baring, M. G., Jones, F. C. & Ellison, D. C. 2004, ApJ 600, 485.
23. Drury, L. O'C. 1983, Rep. Prog. Phys. 46, 973.
24. Drury, L. O'C. & Völk, H. J. 1981, ApJ 248, 344.
25. Eichler, D. 1984, ApJ 277, 429.
26. Ellison, D. C., Baring, M. G. & Jones, F. C. 1995, ApJ 453, 873.
27. Ellison, D. C., Baring, M. G. & Jones, F. C. 1996, ApJ 473, 1029.
28. Ellison, D. C. & Double, G. P. 2002, Astroparticle Phys. 18, 213.
29. Ellison, D. C. & Double, G. P. 2004, Astroparticle Phys. in press, [astro-ph/0408527].
30. Ellison, D. C., Drury, L. O'C., & Meyer, J.-P. 1997, ApJ 487, 197.
31. Ellison, D. C. & Eichler, D. 1984, ApJ 286, 691.
32. Ellison, D. C., Jones, F. C., & Reynolds, S. P. 1990, ApJ 360, 702.
33. Ellison, D. C., Möbius, E. & Paschmann, G. 1990 ApJ 352, 376.
34. Forman, M. A., Jokipii, J. R. & Owens, A. J. 1974 ApJ 192, 535.
35. Gallant, Y. A. & Achterberg, A. 1999, M.N.R.A.S. 305, L6.
36. Greisen, K. 1966, Phys. Rev. Lett. 16, 748.
37. Hayashida, N., et al. 1994, Phys. Rev. Lett. 73, 3491.
38. Heavens, A. F. & Drury, L. O'C. 1988, M.N.R.A.S. 235, 997.
39. Jokipii, J. R. 1987, ApJ 313, 842.
40. Jokipii, J. R., Kóta, J. & Giacalone, J. 1993, Geophys. Res. Lett. 20, 1759.
41. Jones, F. C. & Ellison, D. C. 1991, Space Sci. Rev. 58, 259.
42. Jones, F. C., Jokipii, J. R. & Baring, M. G. 1998, ApJ 509, 238.
43. Kennel, C. F. & Coroniti, F. V. 1984, ApJ 283, 694.
44. Kirk, J. G., Guthmann, A. W., Gallant, Y. A., Achterberg, A. 2000, ApJ 542, 235.
45. Kirk, J. G. & Schneider, P. 1987a, ApJ 315, 425.
46. Kirk, J. G. & Schneider, P. 1987b, ApJ 322, 256.
47. Kirk, J. G. & Webb, G. M. 1988, ApJ 331, 336.
48. Lucek, S. G. & Bell, A. R. 2000, M.N.R.A.S. 314, 65.
49. Malkov, M. A. 1997, ApJ 485, 638.
50. Malkov, M. A. & Drury, L. O'C. 2001, Rep. Prog. Phys. 64, 429.
51. Medvedev, M. V. & Loeb, A. 1999, ApJ 526, 697.
52. Meli, A. & Quenby, J. J. 2003, Astroparticle Phys. 19, 649.
53. Mészáros, P. 2002, Ann. Rev. Astron. Astr. 40, 137.
54. Milgrom, M. & Usov, V. 1995, ApJ 449, L37.
55. Nagano, M. & Watson, A. A. 2000, Rev. Mod. Phys. 72, 689.
56. Nishikawa, K.-I., et al. 2003, ApJ 595, 555.
57. Ostrowski, M. 1988, M.N.R.A.S. 233, 257.
58. Ostrowski, M. 1991, M.N.R.A.S. 249, 551.
59. Peacock, J. A. 1981, M.N.R.A.S. 196, 135.
60. Schneider, P. & Kirk, J. G. 1987, ApJ 323, L87.
61. Scully, S. T. & Stecker, F. W. 2002, Astroparticle Phys. 16, 271.
62. Silva, L. O. et al. 2003, ApJ 596, L121.
63. Vietri, M. 1995, ApJ 453, 883.
64. Watson, A. A. 2000, Phys Rep. 333, 309.
65. Waxman, E. 1995, Phys. Rev. Lett. 75, 386.
66. Zatsepin, Z. T. & Kuz'min, V. A. 1966, Zh. Eksp. Teor. Fiz. Pis'ma Red. 4, 144.